NOVEL MONONUCLEAR ZINC(II) COMPLEX WITH NIACIN: CRYSTAL STRUCTURE, DNA/PROTEIN INTERACTION, AND CYTOTOXICITY STUDIES**

C. Zhao [1], L. Huang [2], Q. Wang [1]*

[1] School of Pharmacy, Yancheng Teachers' University, Yancheng, Jiangsu, 224051, China; e-mail: wangqm@yctu.edu.cn
[2] Department of Thoracic Surgery, Yancheng City No.1 People's Hospital, Yancheng, Jiangsu, 224005, China

*A new mononuclear zinc(II) complex $Zn(niacin)_2(H_2O)_4$ (**1**) is synthesized. The interaction of **1** with calf thymus-DNA is investigated by UV-Vis and fluorescence spectrometry, and the apparent binding constant (K_{app}) value is established as 4.6×10^5 M^{-1}. It is found that the quenching mechanism between bovine serum albumin and **1** might be a static quenching procedure with one binding site. Further, the anticancer activity of the complex on three human tumor cells lines (HT29, HepG2, and MCF-7) is studied. The IC_{50} values of **1** on HT29, HepG2, MCF-7 are 114.1±8, 146.7±14, and 319.2±13 μM, respectively.*

Keywords: *zinc(II) complexes, crystal structure, DNA binding, protein binding, anticancer activity, circular dichroism.*

ИЗУЧЕНИЕ КРИСТАЛЛИЧЕСКОЙ СТРУКТУРЫ, ВЗАИМОДЕЙСТВИЯ ДНК/БЕЛОК И ЦИТОТОКСИЧНОСТИ МОНОНУКЛЕАРНОГО КОМПЛЕКСА ЦИНКА(II) С НИАЦИНОМ

C. Zhao [1], L. Huang [2], Q. Wang [1]*

УДК 543.42;535.371

[1] Фармацевтическая школа Яньчэнского педагогического университета, Яньчэн, Цзянсу, 224051, Китай; e-mail: wangqm@yctu.edu.cn
[2] Народная больница № 1 города Яньчэн, Яньчэн, Цзянсу, 224005, Китай

(Поступила 3 ноября 2020)

*Синтезирован новый одноядерный комплекс цинка(II) $Zn(ниацин)_2(H_2O)_4$ (**1**). Взаимодействие комплекса **1** с ДНК тимуса теленка исследовано с помощью УФ-видимой и флуоресцентной спектрометрии. Установлена константа связывания $K_{app} = 4.6\times10^5$ M^{-1}. Показано, что механизм тушения флуоресценции бычьего сывороточного альбумина в присутствии комплекса **1** может быть статическим гашением с одним местом связывания. Исследована противораковая активность комплекса на трех линиях опухолевых клеток человека (HT29, HepG2 и MCF-7). Значения IC_{50} комплекса **1** для HT29, HepG2, MCF-7 составляют 114.1±8, 146.7±14 и 319.2±13 мкМ соответственно.*

Ключевые слова: *комплексы цинка(II), кристаллическая структура, связывание ДНК, связывание с белками, противораковая активность, круговой дихроизм.*

**Full text is published in JAS V. 88, No. 6 (http://springer.com/journal/10812) and in electronic version of ZhPS V. 88, No. 6 (http://www.elibrary.ru/title_about.asp?id=7318; sales@elibrary.ru).

Introduction. It is well known that metal complexes are an important class of compounds endowed with biological interest for their natural propensity to interact with DNA/BSA [1–8]. Metal complexes have been widely studied and have potential applications in the design of therapeutic agents, probing of the DNA specific structures [9–11], and so on. Many studies have focused on the design of inorganic complexes as growth inhibitors of human cancer cells. It has been reported that the only commonly used drugs for the first-line treatment of cancer cells are platinum-based anticancer drugs such as cisplatin, carboplatin, and oxaliplatin [12–17]. Unfortunately, the severe side effects or resistance to platinum-based anticancer drugs cannot be avoided. Therefore, attempts have been made to rationally design metal-based potential anticancer drugs to overcome side effects. Recently, many new types of composite materials have been developed. These complexes are based on different metals and various ligands, combining therapeutic properties and reducing side effects by increasing bioavailability and selectivity.

DNA is one of the widely accepted biological targets for metal-based anticancer agents *in vivo*. There are many interactions between DNA and complexes, such as electrostatic interaction, strong covalent bonding, cleavage of DNA, groove binding, hydrogen-bonding with ligands, DNA intercalation [18–20]. Following the interactions, a lot of metal-based complexes could be exploited for therapeutic purposes. The association between DNA binding and cytotoxic activity remains a crucial step in the search for new anticancer drugs. As effective DNA complexes with potential cytotoxic activity, the development of new metal complexes has attracted more attention. Besides, x-protein has been employed as a model protein for biophysical, biochemical, and physicochemical researches. It is important to study the properties of the binding variety of hydrophobic ligands [21]. Serum albumin is the most abundant protein in plasma, and it plays a leading role in drug allocation and drug efficiency [22]. The most important property of this group of proteins is to act as transporters in the blood. Bovine serum albumin (BSA) is the most widely studied for the structural homology of human serum albumin (HSA) [22–24].

It has been reported that a number of metal-based complexes have received intense interest. Among them we should note zinc complexes as effective DNA binders with potential anticancer activity. Besides, zinc is a significant biological metal that plays a crucial part in human life. Zinc is present in more than 300 enzymes of living organisms [25]. It is reported that Zn(II) derivatives could have potential against cancer with low toxicity and side effects. There are new modes of action and cellular targets for Zn(II) derivatives compared with the classical metallodrugs.

Our previous studies have shown that many platinum and copper complexes can potently interact with DNA/BSA [26]. Zinc, in contrast to platinum and copper, is a more nutritionally essential element. So, the effect of zinc complexes on DNA/BSA is much more physiologically relevant and the observations of the biological effects of the platinum and copper complexes give a demonstration of effects that zinc complexes might have. In this report, a new complex of zinc carboxylic acid was synthesized and characterized. The interactions with DNA/BSA were assessed and compared with those of platinum and copper complexes. The results showed that the zinc complex ***1*** could interact with DNA/BSA. Furthermore, the cytotoxicity and preliminary apoptotic of complex ***1*** were tested.

Experimental. Bovine serum albumin, ethidium bromide (EB), pBR322 DNA, and calf thymus DNA (CT-DNA) were purchased from Sigma used without further purification. The other chemical solvents were purchased from the China Reagent Network and distilled by the standard methods before use.

IR spectra were determined by a Nicolet 380 spectrometer in the range from 4000 to 400 cm^{-1}. Electrospray ionization mass spectrometry (ESI-MS) was recorded on a Triple TOFTM 5600^+ system with an ion spray source in the positive-ion mode. Electronic spectra were obtained by means of a Hewlett Packard HP-8453. Fluorescence spectral data were received on a RF-5301 fluorescence spectrophotometer at the approved temperature.

X-ray crystallographic data were collected on a Rigaku Saturn X-ray CCD diffractometer using MoK_α radiation (λ = 0.71073 Å) with the ω-2θ scan technique at 296(2) *K*. The original strength was corrected by experiential absorption. The structures were solved by direct methods (SHELXS-97) [27–29] and refined by the full-matrix least-squares based on $|F|^2$ using the SHELXTL program package. The non-H atoms were refined to anisotropy. The hydrogen atoms attached to C were considered to be attached to the related atom. The final cycle of the full matrix least-squares subdivision period was based on the observed reflection and variable parameters. The crystal structure was checked for higher symmetry using PLATON. The details of the crystallographic data for complex ***1*** are given in Table 1. The crystallographic data for the structures was deposited at the Cambridge Crystallographic Data Centre, CCDC Nos. 1851283 for ***1***.

TABLE 1. Crystallographic Data for Complex ***1***

Empirical formula	$C_{12}H_{16}N_2O_8Zn$	*a* (Å)	14.1693(5)
CCDC	1851283	*b* (Å)	6.8883(3)
Formula weight	381.64	*c* (Å)	8.4682(3)
Temperature	296(2) K	α (°)	90
Wavelength	0.71073 A	β (°)	118.175(2)
Crystal system	monoclinic	γ (°)	90
space group	C2	V (Å^3)	728.58(5)
Z	2	R_{int}	0.1482
D_{calc}(g · cm^{-3})	1.740	R_1, $wR_2[I > 2\sigma(I)]$	0.0537
F(000)	392		0.1270
Goodness of fit	1.304	R_1, wR_2(all data)	0.0658
Completeness (%)	99.6%		0.1671
Reflections collect.	6635	Reflections unique	1696

DNA binding experiments. The titration of the absorption spectra was performed for constant concentrations of zinc(II) complexes (20 μM) with different concentrations of CT-DNA (0–50 μM). The CT-DNA stock solution was prepared with 5 mM Tris-HCl/50 mM NaCl (pH 7.20) and stored at 4°C and used for less than a week. For protein-free CT-DNA, the UV absorbance ratio at 260 to 280 nm should be 1.8–1.9. The concentration of CT-DNA was studied with UV absorbance at 260 nm, which takes 6600 $M^{-1}\cdot cm^{-1}$ as the molar absorption coefficient. From the study of the absorption titration the properties of the equilibrium DNA binding constants K_b were determined by equations that included the binding site [17, 26]:

$$\frac{\varepsilon_a - \varepsilon_f}{\varepsilon_b - \varepsilon_f} = \frac{(b - (b^2 - 2K_b^2 C_t[\mathrm{DNA}]/s)^{1/2})}{2K_b C_t} \quad (1)$$

$$b = 1 + K_b C_t + K_b[\mathrm{DNA}]/2s, \quad (2)$$

where ε_a is the absorption intensity, ε_f is the given DNA concentration, ε_b is the complex absorption intensity when fully bound to DNA(assuming that further increase in DNA does not alter the absorption intensity), K_b is the equilibrium binding constant, C_t is the total DNA concentration, [DNA] is the DNA concentration, and *s* is the size of the binding site. Both K_b and *s* could be obtained by the best fitting line.

Fluorescence spectral studies. A quartz tube with an optical path length of 1 cm was used for the fluorescence emission spectra, and the excitation and emission slits were set at 5 and 5 nm, respectively. An EB fluorescence displacement study was carried out by maintaining a ratio of [DNA]/[EB] = 10. The fluorescence emission spectra were obtained from 530 to 700 nm with increase in the concentration of complex ***1***, the excitation wavelength being 510 nm. In addition, the fluorescence spectra of EB-DNA binding solutions at different concentrations (0–150 μM) were obtained. The synthesized complex ***1*** did not show any fluorescence at the excitation and emission wavelengths. By Eq. (3) we could obtain the apparent DNA binding constant (K_{app}) value:

$$K_{\mathrm{EB}}[\mathrm{EB}] = K_{app}[\mathrm{Complex}]. \quad (3)$$

Bovine serum albumin binding. As our early reports [25, 26], the binding of complex ***1*** with BSA was studied by fluorescence spectra recorded at a fixed excitation wave-length corresponding to BSA at 280 nm and monitoring the emission at 342 nm. In all fluorescence experiments, the excitation and emission slit widths and scan rates were the same. A stock solution of BSA was prepared in 25 mM Tris-HCl buffer (pH 7.2) and stored in the dark at 4 h for further use. A stock solution of the test complex was prepared by dissolving it in DMSO and diluted with Tris-HCl buffer to get the target concentrations. Fluorescence measurements were performed by a RF-5301 fluorophotometer with the concentration of BSA fixed (1.0 μM). The K_{SV}, K_a, and *n* were determined by

$$F_0/F = 1 + k_q\tau_0[Q] = 1 + K_{SV}[Q], \quad (4)$$

$$\log[(F_0 - F)/F] = \log K_a + n\log[Q]. \quad (5)$$

Here F_0 and *F* are the fluorescence intensity in the absence and presence of ***1***, respectively; k_q is the rate constant; K_{SV} is the quenching constant; K_a is the binding constant; τ_0 is the average life expectancy without ***1*** ($\tau_0 = 10^{-8}$ s) [30]; [*Q*] is the concentration of ***1***.

MTT assay. A MTT (3-(4,5-dimethylthiazol-2-yl)-2,5-diphenyltetrazolium bromide) assay was performed in the same way following the reported method [31], and the percentage of cell viability was determined by spectrophotometric determination of the accumulated formazan derivative in treated cells at 590 nm in comparison with the untreated ones. Complex ***1*** (0, 5, 10, 40, 80, 160, and 320 μM) in DMSO was added to the wells containing 1×10^4 cells per well and seeded in 200 mL of a fresh medium for 24 h. DMSO was used as the control. After 24 h, we added 20 mL 5 mg/mL of MTT solution in PBS to each well and wrapped the plates with aluminum foil, followed by incubation for 4 h at 37°. The formazan crystals were air dried in a dark place and dissolved in 100 μL DMSO, and then mildly shaken at room temperature, after which an enzyme-linked immunosorbent assay (ELISA) reader was used to measure the absorbance at 590 nm.

The absorbance values of the percentage cell growth calculated from equation

$$\text{Percentage growth} = 100\times(T - T_0)/(C - T_0), \quad (6)$$

where T is the absorbance of ***1*** treated cell (HepG2, MCF7, and HT29); C is the absorbance of control cells; T_0 is the absorbance at time zero.

Synthesis of the complex *1*. Complex ***1*** $Zn(niacin)_2(H_2O)_4$ was prepared by the reported method with some modification [32, 33]. Zinc chloride (136.3 mg, 1.0 mmol) was dissolved in water (10 mL) and niacin (369.3 mg, 3.0 mmol), methanol (10 mL) was added, and the reaction mixture was stirred for about 3 h. Then colorless crystals of *1* were obtained (yield 37.4%) within a week. Elemental analysis for $Zn(niacin)_2(H_2O)_4 \cdot 0.3H_2O$: calculated: C% 45.38, H% 2.77, N% 8.83; found: C% 45.44, H% 2.83, N% 8.82. IR (cm^{-1}): 3218s ν(O–H), 1685 m ν(C=O), 565m ν(Zn-N), 623m ν(Zn-O) (s, strong; m, medium; w, weak). Electrospray ionization mass spectrometry (ESI-MS): *m*/*z* 380.0209 $[1 + Na]^+$ 403.0131.

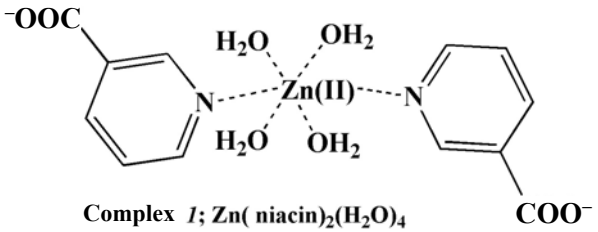

Complex *1*; $Zn(niacin)_2(H_2O)_4$

IR, EAs, and Mass spectral (ESI-MS) and X-ray single crystal diffraction was used to characterize the structure of complex ***1***. By comparing the IR of ***1*** with the free ligand, we found that there were expected differences between them due to the formation of different coordination bonds. ESI-MS manifested that the structure of complex ***1*** is the same as for our design. X-Ray single crystal diffraction clearly proved that ***1*** had been successfully synthesized by us.

The stability of ***1*** was investigated by ESI-MS in the DMSO system. Besides, 10^{-2} M of ***1*** in the DMSO solution was diluted by 5 mM Tris-HCl buffer to obtain the 10^{-4} M of ***1***, the UV-Vis was used to further confirm the stability of ***1*** in the assay buffer. The UV-Vis data showed that there were no obvious changes for ***1*** indicating that ***1*** is stable enough in the assay system and the ligand isonicotinic acid may not be released from complex ***1***.

The crystal structure of ***1*** is shown in Fig. 1, the central Zn(II) ions exhibited octahedron geometry. Four of six-coordinated positions are filled with four O (O3, O3A, O4, O4A) atoms which comes from the water of the solvent. The base of the octahedron is made up by O3, O3A, O4, O4A, and the Zn1 is located at the center of the base. The other two sites are in the axial position occupied by nitrogen atoms of niacin. From Table 2 one can see that the distances of Zn1-O3 and Zn1-O4 are 2.123(6) and 2.132(6) Å, respectively. The Zn-N bonds in the axis of the octahedron are normal with the distances being 2.148(3) and 2.148(3) Å, respectively. The Zn-N bond is longer than other reports, which indicated that Zn-N bond distances lie in the range of 2.0606(15)–2.074(3) Å [16] while the Zn-O bonds are similar to the early results.

The packing patterns of mononuclear units in complex ***1*** are listed in Fig. 2. In complex ***1*** adjacent mononuclear units are linked by O-H···O hydrogen bonds between water oxygen atoms and carbonyl oxygen atoms, while C–H...O between the pyridine ring of niacin and water oxygen atoms, O–H···O hydrogen bonds between water oxygen atoms and carbonyl oxygen atoms generate infinite 2D planes (Fig. 2 and Table 3).

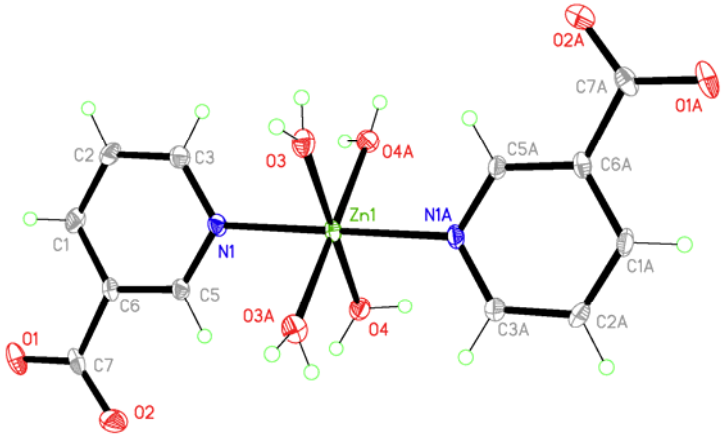

Fig. 1. X-ray structure of complex ***1*** with a 30% probability of thermal ellipsoids.

TABLE 2. Bond Lengths (Å) and Bond Angle (°) for Complex ***1***

Zn1-O3	2.132(6)	Zn1-O4	2.123(6)
Zn1-O3_$1	2.132(6)	Zn1-O4_$1	2.123(6)
Zn1-N1	2.356(7)	Zn1-N1_$1	2.148(3)
O4-Zn1-O3	179.8(3)	O4-Zn1-N1	88.7(2)
O3-Zn1-N1	91.5(2)	C5-N1-Zn1	120.51(19)
C3-N1-Zn1	122.0(2)	N1-Zn1-N1_$1	179.3(5)
O3-Zn1-N1_$1	91.5(2)	O3-Zn1-N1_$1	89.0(2)
O4-Zn1-N1_$1	90.8(2)	O4-Zn1-N1_$1	88.7(2)
O3-Zn1-N1_$1	89.0(2)	O4-Zn1-O4_$1	88.9(3)
O4-Zn1-O3_$1	91.17(11)	O4-Zn1-O3_$1	179.8(3)
O4-Zn1-O3_$1	91.17(11)	O3-Zn1-O3_$1	88.8(3)
O4-Zn1-N1_$1	90.8(2)		

N o t e: Symmetry trans formations used to generate equivalent atoms: $ 1 –*x*, *y*, –*z*.

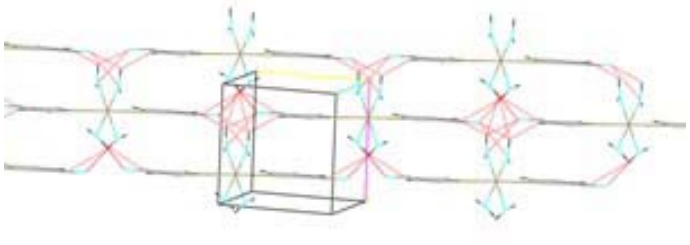

Fig. 2. Hydrogen bonds network for complex ***1***.

TABLE 3. Hydrogen Bonds for Complex ***1***

D-H...A	*d*(D-H)	*d*(H...A)	*d*(D...A)	<(DHA)
O3-H3W...O1_$2	1.05	2.11	2.706(9)	114.1
O4-H4W...O1_$3	0.87(5)	1.83(5)	2.703(9)	175(4)
O4-H4...O2_$4	0.82	1.98	2.713(7)	148.8
O3-H3...O2_$5	0.82	1.92	2.685(8)	153.7
C5-H5...O2	0.93	2.41	2.749(4)	101

N o t e: Symmetry trans formations used to generate equivalent atoms: $1 –*x*, *y*, –*z*; $2 –*x*+1/2, *y*–1/2, –*z*+1; $3 *x*–1/2, *y*+1/2, *z*–1; $4 –*x*, *y*, –*z*+1; $5 *x*, *y*, *z*–1.

DNA is the main intracellular target of anticancer complexes, and the possible interactions between them can lead to DNA damage of cancer cells blocking cancer cells, leading to cell death [34, 35]. Different spectroscopic techniques were used to study the effect of a drug binding to DNA [36]. Electronic absorption spectroscopy, fluorescence spectra and circular dichroism (CD) are the most useful techniques for studying the interactions between the metal complex and DNA. The absorption spectra of ***1*** with CT-DNA are illustrated in Fig. 3a and a plot of $(\varepsilon_a - \varepsilon_f)/(\varepsilon_b - \varepsilon_f)$ versus [DNA] for the titration of DNA to ***1*** is shown in Fig. 3a, inset. A peak at 270 nm of ***1*** could be attributed to intraligand π-π* transition. An increase in the molar absorptivity for ***1*** was found when the CT-DNA concentration increased. It is investigated that the intercalative mode was involved when ***1*** bound to DNA [37, 38]. The intrinsic binding constant K_b was obtained by Eq. (1) and (2), and the value was 1.4×10^5 M^{-1}, which is superior to our early report [25, 26]. Besides, the medium binding strength of complex ***1*** with CT-DNA was obtained from the binding constant.

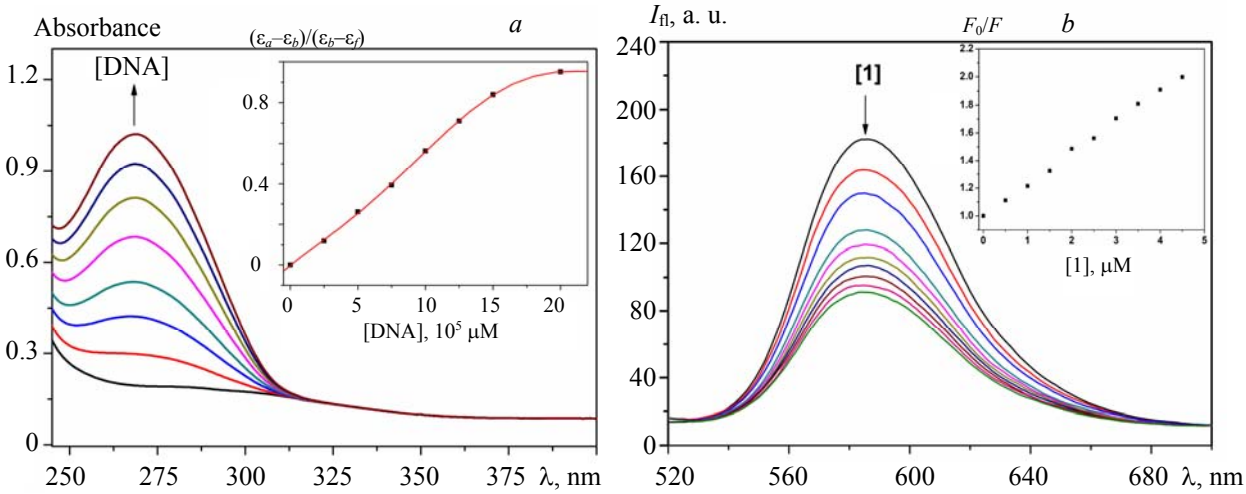

Fig. 3. a) Absorption spectra of complex ***1*** (10 μM) in the absence (black line) and presence (color line) of CT-DNA with concentration 0, 2.5, 5.0, 7.5, 10.0, 12.5, 15.0, and 20.0 μM in 5 mM Tris-HCl/50 mM NaCl buffer (pH 7.2). Inset: Plot of $(\varepsilon_a - \varepsilon_f)/(\varepsilon_b - \varepsilon_f)$ versus [DNA] for the titration of DNA to ***1***. b) Fluorescence emission spectra of EB-CT-DNA in the absence (black line) and in the presence (color lines) of ***1*** with concentration 0, 0.5, 1.0, 1.5, 2.0, 2.5, 3.0, 3.5, 4.0, and 4.5 μM. Inset: plot of F_0/F versus [***1***] shows linearity.

EB (ethidium bromide) is a classical intercalator, and its fluorescence intensity could be increased under complexing with DNA [39]. With the fluorescence spectral technique, we determined the apparent binding constant (K_{app}) of ***1*** with DNA. Due to the strong intercalation of EB between the adjacent DNA base pairs, strong fluorescence is found, which could be quenched by the addition of another molecule [40]. In order to determine the binding mode of ***1*** with CT-DNA, a competitive EB replacement test was carried out. The fluorescence emission intensity of EB bound to CT-DNA was monitored in 5 mM Tris-HCl/50 mM NaCl buffer (pH 7.20). From Fig. 3b it is evident that when ***1*** is added, a considerable fluorescence intensity decrease of the EB-DNA is found, indicating that the EB is replaced by ***1*** from their DNA binding sites. From Eq. (3) we could calculate the apparent binding constant (K_{app}), and the K_{app} values for ***1*** is 4.6×10^5 M^{-1}. Such K_{app} value indicates that ***1*** is bound to DNA by intercalation.

MTT assay is a colorimetric method based on the conversion of yellow tetrazolium salt into purple formazan crystals by metabolically active cells. So, the cytotoxic effects of ***1*** on the viability of several human cancer cell lines (HT29, HepG2, and MCF-7) were investigated by MTT assay. We put various tumor cells in ***1*** of different concentrations and then incubated for 48 h (the concentration of ***1*** were 0, 25, 50, 100, and 300 μM). We observed that ***1*** is cytotoxic to the tested cancer cells, and the growth of cells in a dose-dependent manner could be inhibited (Fig. 4). So, complex ***1*** is a potential anticancer agent for HepG2 and MCF-7 cells with the IC_{50} value of 114.1±8 and 146.7±14 μM, respectively. The present complex *1* exhibited the same in vitro cytotoxicity against tested cancer cell lines as tridentate copper(II) complexes [41]. Moreover, the cytotoxicity of ***1*** to HepG2 cells in vitro was higher than that of 5-fluorouracil, an antitumor drug widely used in clinic, but lower than that of cisplatin.

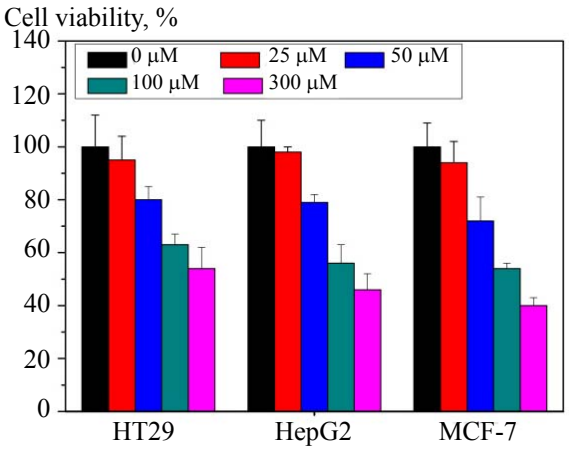

Fig. 4. Cell viability of MCF-7, HepG2 and HT29 cells treated with complex ***1*** at 0, 25, 50, 100, 200, and 300 μM for 48 h.

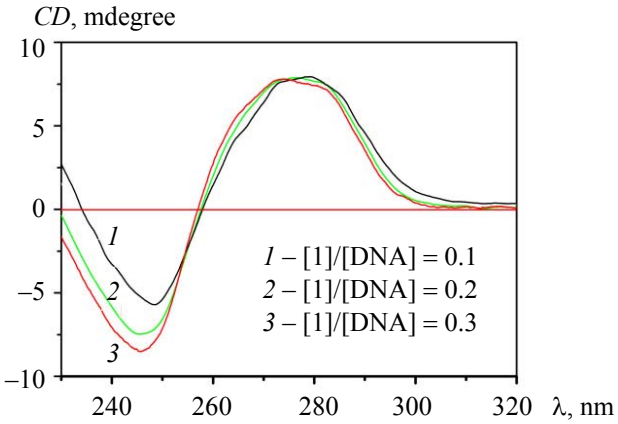

Fig. 5. Circular dichroism spectra of CT-DNA before and after reaction with complex ***1*** at the [***1***]/[DNA] ratios given in the figure.

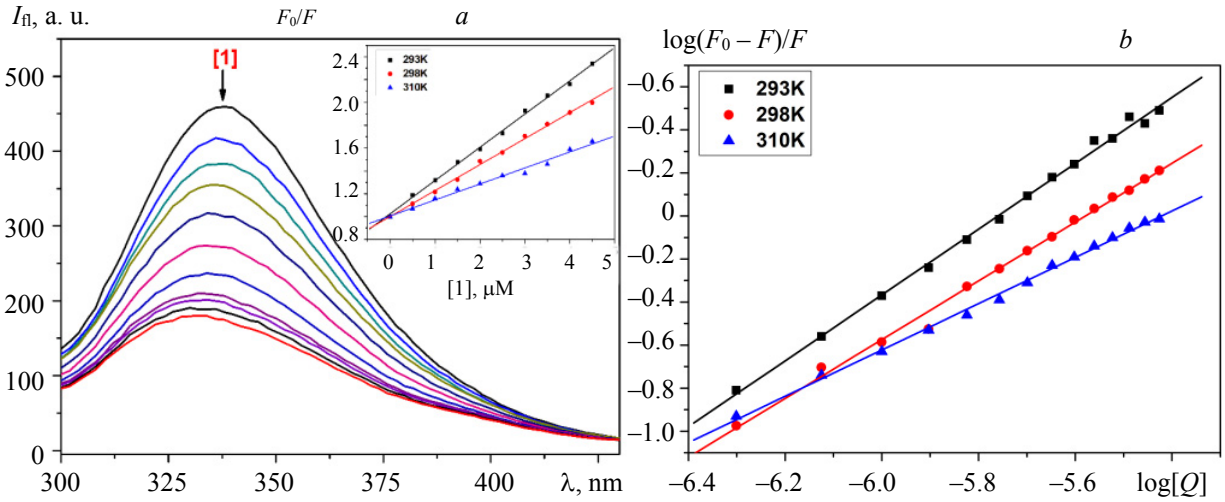

Fig. 6. (a) Fluorescence emission spectra of BSA (1.0 μM) in the absence and presence of complex ***1*** with concentrations 0.25, 0.5, 0.75, 1.0, 1.25, 1.5, 1.75, 2.0, and 2.25 μM. Inset: plot of F_0/F versus [***1***]; b) Plot of $\log(F_0 - F)/F$ vs. $\log[Q]$ for BSA in the presence of ***1***.

The CD spectra of CT-DNA and those obtained in the presence of complex ***1*** are observed in Fig. 5. As seen, the positive band registered at 276 nm shows no obvious increase or decrease, which corresponds to values of [***1***]/[DNA] ranging between 0.1 and 0.3. The negative band registered at 245 nm shows an enhancement with the increase in the [***1***]/[DNA] ratio. A higher [***1***]/[DNA] ratio produces a decrease in the positive band accompanied by significant hypochromatic changes [42]. Two isodichroic effects are observed at values of the [***1***]/[DNA] ratio between 0.1 and 0.3. The results obtained in this study differed from those reported for CT-DNA-cisplatin CD [43, 44].

Similarly, complexes may also interact with proteins (YSA, BSA, et al.) [45, 46]. From Fig. 6a one can see a strong fluorescence emission peak at 340 nm of BSA. It decreased when ***1*** was gradually added. We could estimate the quenching type between ***1*** and BSA by the Stern-Volmer formula [40]. Table 4 presents a list of the values of K_{SV} and k_q for the interaction of ***1*** with BSA.

From Table 4 we found that k_q was 18.6×10^{12} $M^{-1}\cdot s^{-1}$ for the interaction of ***1*** with BSA. Owing to this, the quenching is static [47]. The binding constants and binding sites were calculated by Eq. (5). Thus, K_a was the apparent binding constant, while n was the binding site (as shown in Fig. 6b). The calculated cumulative binding constants K_a from the data were $K_a = 6.24\times10^5$ at 293 K, $K_a = 5.76\times10^5$ at 298 K, and $K_a = 3.82\times10^5$ at 310 K, respectively. The binding constants K_a and binding sites n of complex ***1*** and BSA at different temperature can be obtained and are listed on Table 4.

TABLE 4. The Quenching Constants (K_{SV}), Binding Constants (K_a), and Binding Sites (n) of BSA-1 at Different Temperature

Temperature, K	$K_{SV}\times10^5$, M^{-1}	$K_q\times10^{12}$, M^{-1}	$K_a\times10^5$, M^{-1}	n
293	2.91	29.1	6.24	0.96
298	2.27	22.7	5.16	1.07
310	1.42	14.2	3.82	1.02

Usually, the thermodynamic parameters such as enthalpy change (ΔH) and entropy change (ΔS) are used for finding the interaction force. The ΔH could be regarded as a constant with the temperature changes. Thermodynamic parameters can be determined from the equation, which is derived from the van't Hoff equation:

$$\ln(K_2 / K_1) = \frac{\Delta H}{R}\ \frac{T_2 - T_1}{T_1 T_2}. \quad (7)$$

The Gibbs free energy change (ΔG) could be obtained from formula

$$\Delta G = -R\mathrm{T}\ln K = \Delta H - T\Delta S, \quad (8)$$

where R is the gas constant.

Table 5 presents the thermodynamic parameters. Due to the negative value of ΔH, ΔG and the positive value of ΔS, we could indicate that the formation of ***1*** and BSA is a spontaneous and exothermic reaction. Different signs of the thermodynamic parameters associated with various types of interactions can be observed in protein association processes [48]. The hydrophobic interactions were characterized by the positive value of ΔS, and the hydrogen bonds and the van der Waals force were characterized by the negative value of ΔH.

TABLE 5. Thermodynamic Parameters of BSA Complexing with Complex ***1***

Temperature, K	293	298	310
K_a	6.24	5.16	3.82
ΔH, KJ/mol	–12.05	–12.05	–12.05
ΔG, KJ/mol	–32.51	–32.87	–34.55

In summary, a zinc complex, $Zn(niacin)_2(H_2O)_4$ (***1***) was synthesized and characterized, and its interaction with DNA/BSA was also investigated. The binding properties of ***1*** to DNA were investigated by electron absorption, fluorescence spectroscopy, and circular dichroism. The results confirmed that the interaction of ***1*** and CT-DNA was by intercalation and the binding strength was medium with the binding constant 4.6×10^5 M^{-1}. Moreover, the ability to bind to BSA was also investigated, and the quenching static mecha-

nism of ***1*** and BSA was established. Besides, the in vitro cytotoxic activities revealed that ***1*** could inhibit the selected tumor cell lines (HT29, HepG2, and MCF-7). The thermodynamic parameters indicated that the hydrophobic bond, hydrogen bond, and the van der Waals force play a dominant role in the binding process. These results indicated that the promoted interactions were found between ***1*** and CT-DNA.

Acknowledgements. This work financially supported by the practice innovation training program projects for the Jiangsu College students (201910324006Y), the Natural Science Foundation of the Jiangsu Higher Education Institutions of China (20KJA150003), and the Studying Abroad Scholarships of Yancheng Teachers University.

REFERENCES

1. K. B. Garbutcheon-Singh, M. P. Grant, B. W Harper, A. M. Krause-Heuer, M. Manohar, N. Orkey, J. R. Aldrich-Wright, *Curr. Top. Med. Chem.*, **11**, 521–542 (2011).
2. G. Y. Li, R. L. Guan, L. N. Ji, H. Chao, *Coord. Chem. Rev.*, **281**, 100–113 (2014).
3. A. C. Komor, J. K. Barton, *Chem. Commun*., **49**, 3617–3630 (2013).
4. R. Senthil Kumar, S. Arunachalam, *Polyhedron*, **26**, 3255–3262 (2007).
5. F. Xue, C. Z. Xie, Y. W. Zhang, Z. Qiao, X. Qiao, J. Y. Xu, S. Y. Yan, *J. Inorg. Biochem.*, **115**, 78–86 (2012).
6. X. F. Zhao, Y. Ouyang, Y. Z. Liu, Q. J. Su, H. Tian, C. Z. Xie, J. Y. Xu. *New J. Chem*., **38**, 955–965 (2011).
7. W. J. Lian, X. T. Wang, C. Z. Xie, H. Tian, X. Q. Song, H. T. Pan, X. Qiao, J. Y. Xu, *Dalton Trans*., **45**, 9073–9087 (2016).
8. C. Y. Gao, Z. Y. Ma, Y. P. Zhang, S. T. Li, W. Gu, X. Liu, J. L. Tian, J. Y. Xu, J. Z. Zhao, S. P. Yan, *RSC Adv.*, **5**, 30768–30779 (2015).
9. K. D. Mjos, C. Orvig, *Chem. Rev*., **114**, 4540–4563 (2014).
10. G. Barone, A. Terenzi, A. Lauria, A. M. Almerico, J. M. Leal, N. Busto, B. García, *Coord. Chem. Rev*., **257**, 2848–2862 (2013).
11. Q. Jiang, N. Xiao, P. Shi, Y. Zhu, Z. Guo, *Coord. Chem. Rev*., **251**, 1951–1972 (2007).
12. J. J. Wilson, S. J. Lippard, *Chem. Rev*., **114**, 4470–4495 (2014).
13. N. Muhammad, Z. Guo, *Curr. Opin. Chem. Biol.*, **19**, 144–153 (2014).
14. A. M. Florea, D. Busselberg, *Cancers*, **3**, 1351–1371 (2011).
15. Z. Y. Ma, Z. Qiao, D. B. Wang, X. Hou, X. Qiao, C. Z. Xie, Z. Y. Qiang, J. Y. Xu, *Appl. Organomet. Chem*., **31**, No. 7, e3651 (2017).
16. X. D. Lin, Y. H. Liu, C. Z. Xie, W. G. Bao, J. Shen, J H. Xu, *RSC Adv*., **7**, No. 42, 26478–26486 (2017).
17. Q. M. Wang, L. Yang, J. H. Wu, H. Wang, J. L. Song, X. H. Tang, *Biometals*, **30**, No. 1, 17–26 (2017).
18. C. H. Leung, H. Z. He, L. J. Liu, M. Wang, D. S. H. Chan, D. L. Ma, *Coord. Chem. Rev*., **257**, 3139–3151 (2013).
19. H. K. Liu, P. J. Sadler, *Acc. Chem. Res*., **44**, 349–359 (2011).
20. Y. Aiba, J. Sumaoka, M. Komiyama, *Chem. Soc. Rev*., **40**, 5657–5668 (2011).
21. O. K. Abou-Zied, *Curr. Pharm. Des.*, 21, 1800–1816 (2015).
22. R. E. Olson, D. D. Christ, *Annu. Rep. Med. Chem*., **31**, 327–336 (1996).
23. J. Maiti, S. Biswas, A. Chaudhuri, S. Chakraborty, S. Chakraborty, R. Das, *Spectrochim. Acta A*, **175**, 191–199 (2017).
24. S. Ghosh, S. Chakrabarty, D. Bhowmik, G. S. Kumar, N. Chattopadhyay, *J. Phys. Chem. B*, **119**, 2090–2102 (2015).
25. V. Kolenko, E. Teper, A. Kutikov, R. Uzzo, *Nat. Rev. Urol.*, **10**, 219–226 (2013).
26. Q. M. Wang, H. Mao, W. L. Wang, H. M. Zhu, L.H. Dai, Y. L. Chen, Xinhui Tang, *Biometals*, **30**, No. 4, 575–587 (2017).
27. G. M. Sheldrick. SADABS, University of Göttingen, Germany (2000).
28. G. M. Sheldrick. SHELXS 97 and SHELXL 97, University of Göttingen, Germany (1997).
29. Bruker, SMART (Version 5.0) and SAINT (Version 6.02), Bruker AXS Inc., Madison, Wisconsin, USA (2000).
30. P. Grzegorz, *Arch Biochem. Biophys*., **453**, 54–62 (1978).
31. J. Carmichael, W. G. DeGraff, A. F. Gazdar, J. D. Minna, J. B. Mitchell, *Cancer Res*., **47**, 936–942 (1978).

32. H. Han, L. P. Lu, Q. M. Wang, M. L. Zhu, C. X. Yuan, S. Xing, X. Q. Fu, *Dalton Trans*., **41**, 111116–111124 (2012).
33. Q. M. Wang, M. L. Zhu, L. P. Lu, C. X. Yuan, S. Xing, X. Q. Fu. *Dalton Trans*., **2011**, 40, 12926–12934.
34. L. E. Ta, L. Laura Espeset, J. Jewel Podratz, A. J. Windebank, *Neurotoxicology*, **27**, 992–1002 (2006).
35. S. Dhar, D. Senapati, P. K. Das, P. Chatopadhyay, M. Nethaji, A. R. Chakravarty, *J. Am. Chem. Soc*., **125**, 12118–12124 (2003).
36. E. R. Jamieson, S. J. Lippard, *Chem. Rev*., **99**, 2467–2498 (1999).
37. S. S. Bhat, A. A. Kumbhar, H. Heptullah, A. A. Khan, V. V. Gobre, S. P. Gejji, V. G. Puranik, *Inorg. Chem*., **50**, 545–558 (2011).
38. P. Sevilla, J. M. Rivas, F. GarcÍa-Blanco, J. V. García-Ramos, S. Sánchez-Cortés, *Biochim. Biophys. Acta*, **1774**, 1359–1369 (2007).
39. J. B. LePecq, C. C. Paoletti, *J. Mol. Biol*., **27**, 87–106 (1976).
40. A. Gohel, M. B. McCarthy, G. Gronowicz, *Endocrinology*, **140**, 5339–5347 (1999).
41. G. Y. Li, K. J. Du, J. Q. Wang, J. W. Liang, J. F. Kou, X. J. Hou, L. N. Ji, H. Chao, *J. Inorg. Biochem.*, **119**, 43–53 (2013).
42. A. T. M. Marcelis, J. H. J. Den Hartog, G. A. Van der Marel, G. Wille, J. Reedijk, *Eur. J. Biochem*., **135**, 343–349 (1983).
43. R. C. Srivastava, J. Froehlich, G. L. Eichhorn, *Biochimie*, **60**, 879–891 (1978).
44. J. P. Macquet, J. L. Butour, *Eur. J. Biochem*., **83**, 375–387 (1978).
45. L. Cheng, C. Bulmer, A. Margaritis, *Curr. Drug Deliv*., **12**, 351–357 (2009).
46. X. L. Shi, X. W. Li, M. Y. Gui, H. Y. Zhou, R. J. Yang, H. Q. Zhang, J. R. Jin, *J. Lumin*., **130**, 637–644 (2009).
47. X. J. Guo, L. Zhang, X. D. Sun, X. W. Han, C. Guo, P. L. Kang, *J. Mol. Struct*., **928**, 114–120 (2009).
48. P. D. Ross, S. Subramanian, *Biochemistry*, **20**, 3096–3102 (1978).